European Journal of Medicinal Chemistry 94 (2015) 252–264

Contents lists available at ScienceDirect

European Journal of Medicinal Chemistry

journal homepage: http://www.elsevier.com/locate/ejmech

Original article

General role of the amino and methylsulfamoyl groups in selective cyclooxygenase(COX)-1 inhibition by 1,4-diaryl-1,2,3-triazoles and validation of a predictive pharmacometric PLS model

Maria Grazia Perrone [a, 1], Paola Vitale [a, 1], Andrea Panella [a], Cosimo G. Fortuna [b], Antonio Scilimati [a, *]

[a] Dipartimento di Farmacia – Scienze del Farmaco, Università degli Studi di Bari "A.Moro", Via E. Orabona 4, 70125 Bari, Italy
[b] Dipartimento di Scienze Chimiche, Università degli Studi di Catania, Viale A. Doria 6, 95125 Catania, Italy

ARTICLE INFO

Article history:
Received 31 July 2014
Received in revised form
23 February 2015
Accepted 24 February 2015
Available online 28 February 2015

Keywords:
1,2,3-Triazoles
COX inhibition
Predictive pharmacometric model
Volsurf plus

ABSTRACT

A novel set of 1,4-diaryl-1,2,3-triazoles were projected as a tool to study the effect of both the heteroaromatic triazole as a core ring and a variety of chemical groups with different electronic features, size and shape on the catalytic activity of the two COX isoenzymes. The new triazoles were synthesized in fair to good yields and then evaluated for their inhibitory activity towards COXs arachidonic acid conversion catalysis. Their COXs selectivity was also measured. A predictive pharmacometric Volsurf plus model, experimentally confirmed by the percentage (%) of COXs inhibition at the concentration of 50 μM and IC_{50} values of the tested compounds, was built by using a number of isoxazoles of known COXs inhibitory activity as a training set. It was found that two compounds {4-(5-methyl-4-phenyl-*1H*-1,2,3-triazol-1-yl)benzenamine (**18**) and 4-[1-(4-methoxyphenyl)-5-methyl-1*H*-1,2,3-triazole-4-yl]benzenamine (**19**)} bearing an amino group (NH_2) are potent and selective COX-1 inhibitors (IC_{50} = 15 and 3 μM, respectively) and that the presence of a methylsulfamoyl group (SO_2CH_3) is not a rule to have a Coxib. In fact, 4-(4-methoxyphenyl)-5-methyl-1-[4-(methylsulfonyl)phenyl]-1*H*-1,2,3-triazole (**23**) has COX-1 IC_{50} = 23 μM and was found inactive towards COX-2.

1. Introduction

In the last two decades, the interest around the cyclooxygenases was focused on the inducible isoform COX-2, trying to exalt therapeutic over adverse side effects and because deemed solely responsible of inflammation processes in respect to the "constitutive" isoenzyme COX-1 [1]. In recent years, the attention around the COX-1 has been growing ever more, especially since it was demonstrated that COX-1 isoform, but not COX-2, is overexpressed in several human pathologies. Particularly, COX-1 is expressed at high levels from the early to advanced stages of human epithelial ovarian cancer, skin and colon, and seems to play a specific key role also in cancer progression. As a consequence, COX-1 might be a novel biomarker for early ovarian cancer detection [2], as well as in other cancer types [1].

Moreover, COX-1, being predominantly localized in microglia, emerged as a prominent player in CNS pathologies with a marked neuroinflammatory component [3–7]. Then, COX-1 high selective inhibition rather than COX-2 (by Coxibs, i.e. celecoxib) is more likely to reduce neuroinflammation. Hence, COX-1 inhibitors have been further investigated, in combination with other specific drugs, as part of a therapeutic protocol aimed to prevent and control neurodegenerative diseases with pronounced inflammation, very often first step of neurodegeneration mechanisms [8].

In addition, the use of COX-1 as a theranostic target in many human health problems, is becoming more and more attractive, since it has been proven that its selective inhibition is not responsible of stomach damage [9], the main heavy adverse side effect of NSAIDs.

As a consequence, the development of selective COX-1 inhibitors could be quite important for the treatment and visualization of diseases in which the COX-1 isoenzyme is overexpressed [1].

Very few selective COX-1 inhibitors are currently known, and among those we focused our attention on the diarylheterocycle scaffold.

* Corresponding author.
E-mail address: antonio.scilimati@uniba.it (A. Scilimati).
[1] M. G. Perrone and P. Vitale have equally contributed to this project.

http://dx.doi.org/10.1016/j.ejmech.2015.02.049
0223-5234/

Over the past decade, starting from our lead **P6** [10], [3-(5-chlorofuran-2-yl)-5-methyl-4-phenylisoxazole] (Fig. 1), some diarylheterocycles as COX-1 inhibitors have been prepared. Isoxazole nucleus was deeply investigated by linking to the diarylheterocycle several groups with different features to better identify the COX-1 active site requirements for its efficacious, potent and selective inhibition [11,12].

Triazole has already been used to prepare COXs inhibitors. Most triazoles are known to possess remarkable biological properties such as anti-allergic [13], antibacterial [14], anti-HIV [15] activities and are valuable tools in drug discovery.

Most efforts have been made to develop suitable synthesis of 1,2,4-triazoles endowed with biological activity.

FK881 [3-methoxy-1,5-bis(4-methoxyphenyl)-1*H*-1,2,4-triazole] (Fig. 1) is one of the most studied selective COX-1 inhibitors having the 1,2,4-triazole as a central ring [16]. In view of the various pharmacological properties of the triazole nucleus [17], herein we describe a new series of 1,4-diarylheterocycles bearing the 1,2,3-triazole (regioisomer of 1,2,4-triazole, chemical portion of **FK881**), as a core ring. The novel 1,2,3-triazoles were designed by using a Volsurf plus [18,19] approach, that allowed also to predict their activity as potent and selective COX-1 inhibitors. In order to demonstrate the validity of the Volsurf plus derived pharmacometric model, we prepared and tested the predicted novel 1,4-diaryl-1,2,3-triazoles towards both COX isoenzymes. The structure-inhibitory activity model by Volsurf plus was build also as an attempt to rationalize our previous experimental findings.

The COX inhibitory activity evaluation data confirmed the *in silico* predictions and revealed that in the diarylheterocycle series, the introduction of the 1,2,3-triazole nucleus is not responsible of the COX inhibition; on the contrary, the presence of the NH_2 group somewhere in the molecule is crucial in the selective interaction with COX-1 binding site, as recently found in the isoxazole scaffold [12].

2. Results and discussion

2.1. Design

The 1,2,3-triazole possesses favorable properties in the medicinal chemistry field. It has a moderate dipole character, hydrogen bonding capability, rigidity and remarkable metabolic stability [20]. In addition, 1,2,3-triazole nucleus has been used to reduce the lipophilicity of some Coxibs [21].

COX-1 inhibitors belonging to the diarylheterocycle class are usually tricyclic compounds possessing two aryls bonded to the adjacent atoms of a central heterocycle (Fig. 1). We recently published new COX-1 inhibitors belonging to the class of diarylheterocycles having the aryl groups positioned at C_3 and C_5 of the isoxazole ring (**3t** and **3u**, Fig. 2) and not at C_3/C_4 as usual. In spite of the greater distance between the two aryls, they retain a fair amount of activity as COX-1 inhibitors [22].

On the other hand, 1,2,3-triazoles and their derivatives have emerged as powerful pharmacophores [23], gaining interest for their various biological activities [24–26] as chemotherapeutic agents [27,28], potent antimicrobial [29], anti-inflammatory [30,31], local anaesthetic [32], anticonvulsant [33], antineoplastic [34], antimalarial [35] and antiviral activity [36]. Considering such a biological importance of 1,2,3-triazoles, a new series of the diarylhetherocycles having the aryl groups positioned on N_1 and C_4 of the triazole nucleus was projected to explore further productive and selective interactions with COXs active site.

In addition, a database in which the COX inihibitor activity of eleven isoxazoles, previously published by us [12], was generated with the aim to perform a Quantitative Structure–Activity Relationship (QSAR) investigation using the Volsurf plus (Volsurf+) program. VolSurf plus is an automatic procedure to convert information coded into the 3D GRID Molecular Interaction Fields into 128 physico-chemically relevant molecular descriptors [18,19]. The molecular descriptors obtained refer to molecular size and shape, hydrophilic and hydrophobic properties, hydrogen bonding, amphiphilic moments, critical packing parameters. Moreover, pharmacokinetic descriptors related to solubility, metabolic stability and cell permeability are generated. A complete list of the VolSurf plus descriptors is reported elsewhere [19,37].

A partial least squares regression (PLS) was performed using VolSurf plus, and the model was validated using the Leave One Out (LOO) method.

The eleven compounds of training set and their biological data used to generate the pharmacometric PLS model are listed in Table 1.

A two component PLS model based on the 128 VolSurf plus descriptors was obtained with overall R^2 0.90 and Q^2 0.63. The PLS score plot is depicted in Fig. 3; the background is coloured according to the activity value: blue for active and red (in web version) from inactive. As it is possible to notice, three active compounds previously synthesized were selected in order to verify the goodness of the model and they are, as expected, in the blue region of the plot. The PLS recomputed versus experimental plot of the resulting model is shown in Fig. 4. A significant discrimination between active and inactive compounds was obtained. Compounds are color-coded by their activity values, using a scale from red (actives) to blue (inactives) (in web version).

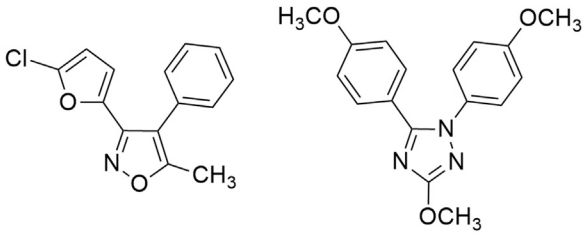

P6

COX-1 IC_{50} = 0.5 μM
COX-2 IC_{50} > 100 μM

FK881

COX-1 IC_{50} = 0.0049 μM
COX-2 IC_{50} = 3.2 μM

Fig. 1. **P6** and **FK881** chemical structure.

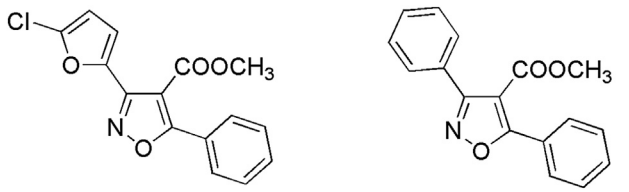

3t

COX-1 IC_{50} = 17.40 μM
COX-2 IC_{50} > 100 μM

3u

COX-1 IC_{50} = 17.28 μM
COX-2 IC_{50} > 100 μM

Fig. 2. Diarylheterocycles as COX-1 selective inhibitors (**3t** and **3u**) with two aryls positioned at the C_3 and C_5 of the isoxazole ring. COXs IC_{50} values are by Human Whole Blood Assay (HWBA) [22].

Table 1
Structures of the eleven compounds used to generate the QSAR model.[a]

Compound code	Structure	COX-1 IC_{50} (% Inhib.)[b]	Compound	Structure	COX-1 IC_{50} (% Inhib.)[b]
P6	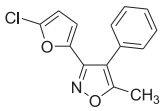	**39 μM** (89)	**MPA7**	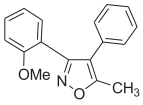	**27 μM** (61)
MPA8	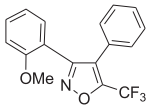	(39)	**MPA9**	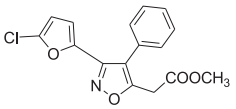	(7)
MPA4	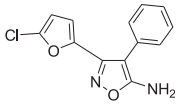	**1.1 μM** (94)	**PM32**	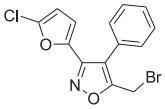	(37)
MPA10	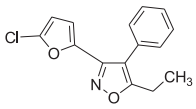	**30 μM** (55)	**PM41**	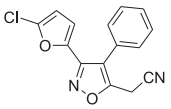	(11)
MPA13	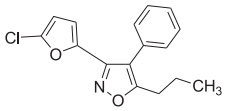	(17)	**MPA15**	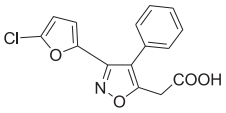	(32)
MPA35	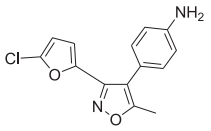	**4 μM** (78)			

[a] Inhibitory activity on *o*COX-1 and *o*COX-2 was determined by using a colorimetric COX (ovine) inhibitor screening assay kit [12].
[b] The percentage (%) of inhibition at 50 μM is reported in the square brackets.

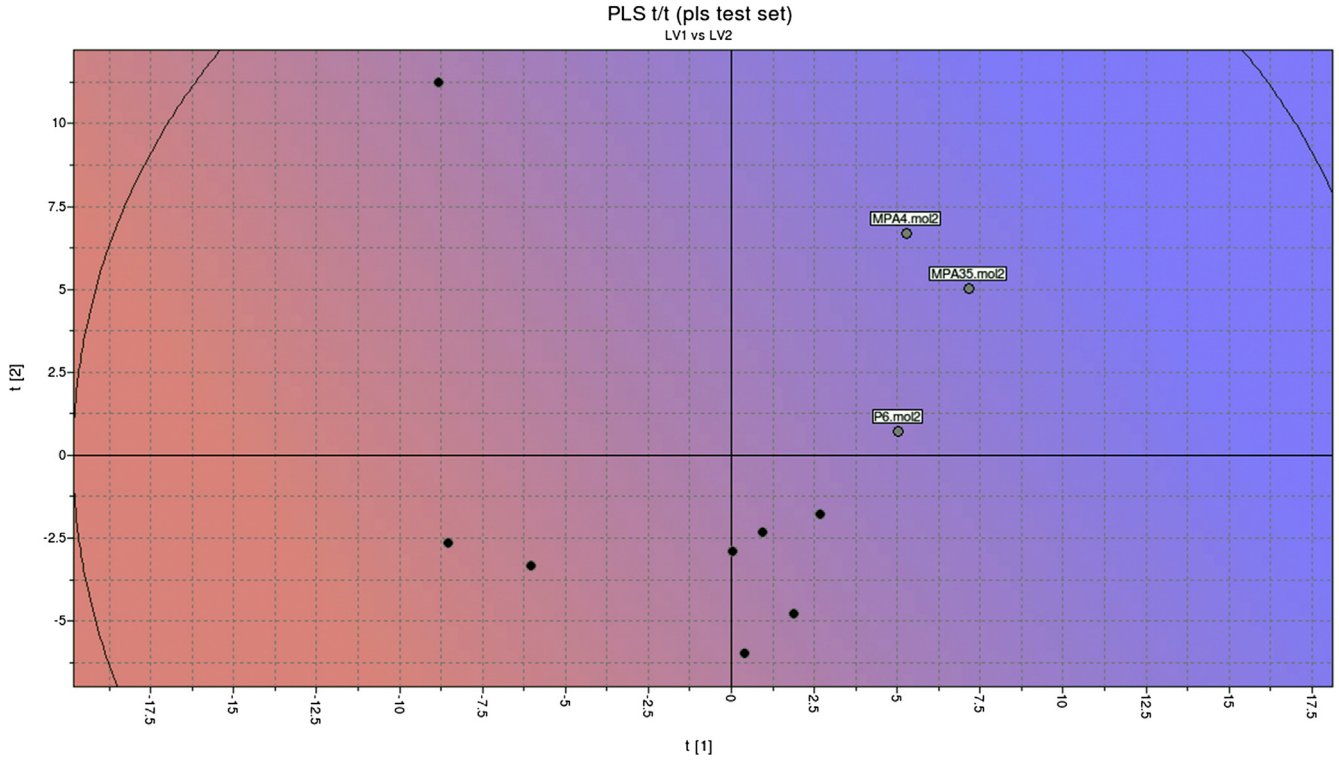

Fig. 3. PLS score plot t1-t2.

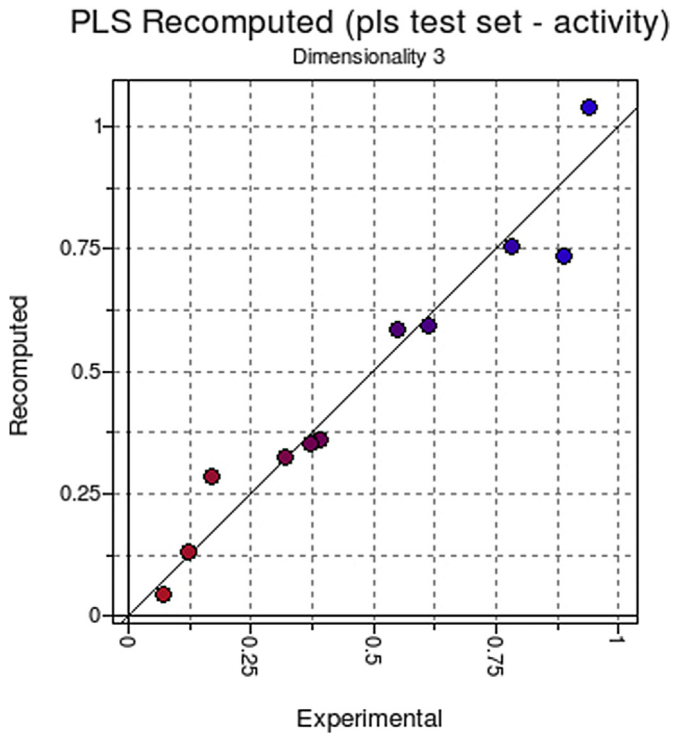

Fig. 4. PLS recomputed versus experimental on t3.

Since the model seems to clearly separate active from inactive compounds, eighteen new 1,2,3-triazoles were designed and projected into the model for activity prediction. A PLS model was obtained in which the first three components explained more than 94.7% of variance.

Fig. 5A–B shows the 3D PLS model after projection of the test-set, and yellow points (in web version) indicate the predicted compounds. Two different prospectives of the same model are reported. In Fig. 5A, some compounds of the training set were selected to evidence the validity of the model. In particular, three isoxazoles reported as active [12] and two reported as inactive were selected. In Fig. 5B, selected yellow point are reported, two predicted as active compounds (**MPA 73** and **MPA 317**, Table 2), that are clustered with the active compounds of the training set (Table 1), and one predicted as inactive (**MPA 333**, Table 2). Probably, the first component (red axis) is discriminant for the activity of 1,2,3-triazoles. In order to demonstrate the validity of the model all the eighteen compounds of the test set were synthesized.

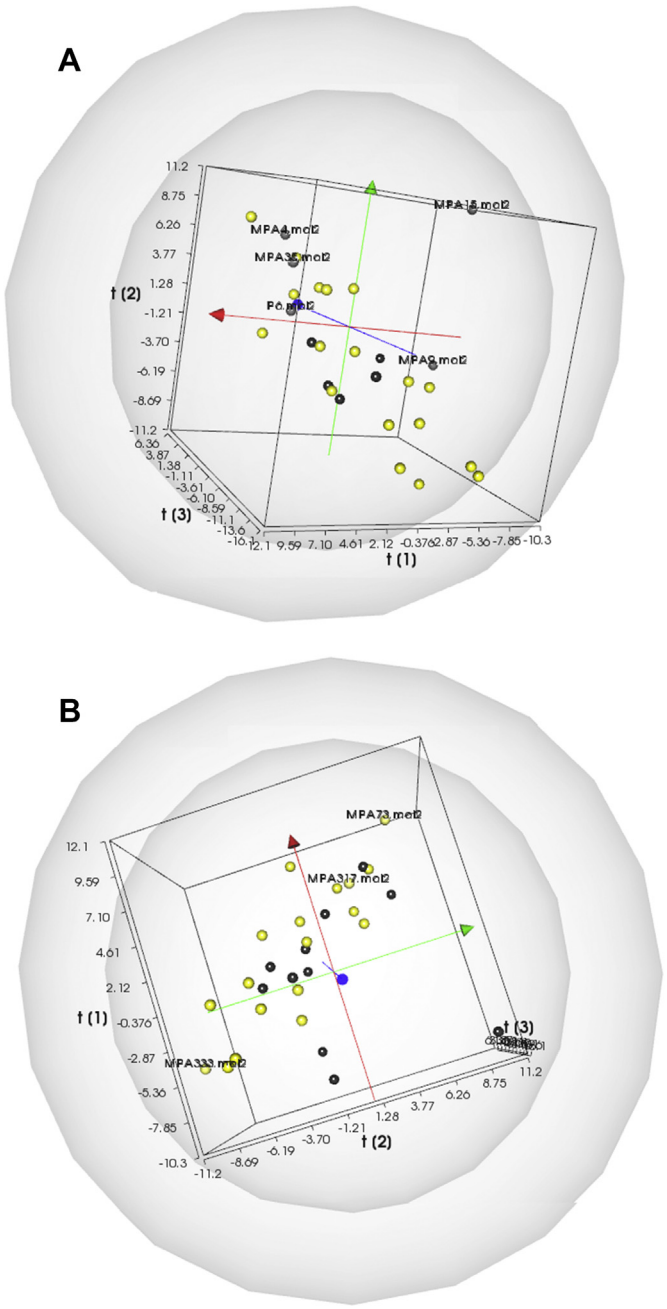

Fig. 5. A–B. Discriminant PLS t1-t2-t3 score plot reporting the projection of the test-set onto the training set PLS model.

2.2. Chemistry

We recently reported the regioselective "one-pot" preparation of 3,4-diarylisoxazoles from reaction of arylnitrile oxides and the sodium enolates of 1-arylpropan-2-one, easily prepared by treating the ketones with NaH in thermodynamic conditions [12,22]. Previously, we also described an efficient two-step procedure for the synthesis of 1-aryl-*1H*-1,2,3-triazoles, based on the reaction of arylazides with the lithium enolate of the acetaldehyde, followed by the dehydration of the hydroxy-triazoline intermediates, under basic conditions [38]. In continuation of our interest in both developing novel heterocycles synthetic methodologies [39,40] and to also study their biological activity, we prepared a series of novel 1,4-diaryl-1,2,3-triazoles by reaction of different arylazides with the enolates of various 1-arylpropan-2-ones.

All the arylazides were prepared in fair to good yields (40–80%) from substituted aryl amines by using *t*-BuONO and moist NaN_3 in *t*-BuOH at room temperature [41] (Scheme 1).

1,3-Diaryl-5-methyl-1,2,3-triazoles **6**–**16** were prepared "one-pot" by 1,3-dipolar cycloaddition of the arylazides (**1**–**5**) to sodium 1-arylpropan-2-one enolates (Scheme 2), obtained, as previously reported by us, by reacting the ketones with NaH at 0 °C. Specifically, 1-(furan-2-yl)propan-2-one sodium enolate reacted with arylazides **3** and **4** to give **14** and **15** (Scheme 2, Table 2).

1-(4-Methoxyphenyl)-5-methyl-4-phenyl-1*H*-1,2,3-triazole (**8**) was demethylated by using BBr_3 in CH_2Cl_2 to prepare the corresponding phenol **17** (Scheme 3).

Reduction reaction of **9** and **11** in the presence of $SnCl_2$ and HCl led to the preparation of 4-(5-methyl-4-phenyl-1*H*-1,2,3-triazol-1-yl)benzenamine (**18**) and 4-(1-(4-methoxyphenyl)-5-methyl-1*H*-

Table 2
COX inhibitory activity of triazoles **6**–**23**.[a,b]

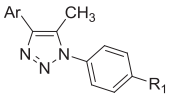

Compound	Ar	R_1	COX-1 % Inhibition (IC_{50})	COX-2 % Inhibition (IC_{50})
6 (MPA 85)	C_6H_5	Cl	n.a.	n.a.
7 (MPA 86)	C_6H_5	F	n.a.	n.a.
8 (MPA 66)	C_6H_5	OCH_3	26	35
9 (MPA 71)	C_6H_5	NO_2	n.a.	n.a.
10 (MPA 125)	C_6H_5	SCH_3	n.a.	14
11 (MPA 302)	4-$NO_2C_6H_5$	OCH_3	20	n.a.
12 (MPA 333)	4-$CH_3SC_6H_5$	OCH_3	n.a.	n.a.
13 (MPA 375)	4-$CH_3OC_6H_5$	OCH_3	25	n.a.
14 (MPA 80)	furan-2-yl-	OCH_3	n.a.	n.a.
15 (MPA 87)	furan-2-yl-	NO_2	n.a.	40
16 (MPA 387)	4-$CH_3OC_6H_5$	SCH_3	n.a.	n.a.
17 (MPA 106)	C_6H_5	OH	n.a.	26
18 (MPA 73)	**C_6H_5**	**NH_2**	**56 (15 μM)**	n.a.
19 (MPA 317)	**4-$H_2NC_6H_5$**	**OCH_3**	**100 (3 μM)**	n.a.
20 (MPA 129)	C_6H_5	SO_2CH_3	21	20
21 (MPA 335)	4-$CH_3SO_2C_6H_5$	OCH_3	20	n.a.
22 (MPA 295)	5-chlorofuran-2-yl-	OCH_3	45	n.a.
23 (MPA 394)	**4-$CH_3OC_6H_5$**	**SO_2CH_3**	**55 (23 μM)**	n.a.

[a] **6**–**23** were screened for their inhibitory activity on COX-1 and COX-2 at 50 μM by using a colorimetric COX (ovine) inhibitor screening assay kit.
[b] n.a. = not active: no inhibitory activity was observed at 50 μM.

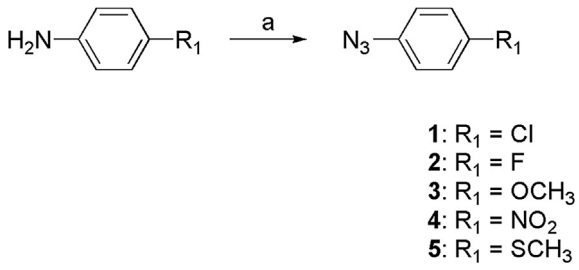

Scheme 1. Reagents and conditions: (a) *t*-BuONO, moist NaN_3, r.t [41].

1,2,3-triazole-4-yl)benzenamine (**19**) (Scheme 4).

10 and **12** CH_3S- moiety was oxidized by *m*-chloroperoxybenzoic acid (*m*CPBA) to the corresponding methylsulfonyl affording **20** and **21** (Scheme 5).

Triazole **14** was treated with *N*-chlorosuccinimide in dry DMF to afford the chlorinated derivative **22** (Scheme 6).

Compound **23** was prepared by sulphur atom oxidation of triazole **16** in the presence of *m*CPBA (Scheme 7).

2.3. COX inhibitory activity

All 1,2,3-triazoles (**6**–**23**) have been tested to exploit their inhibitory behaviour towards both COX-1 and COX-2 isoenzymes (Table 1). A halogen such as Cl and F in **6** and **7**, respectively, did not confer any activity to the molecules. It also occurred in the case of **9** in which the halogen is replaced by the NO_2, a strong electron-withdrawing group (EWG) endowed with -M, -I electronic features. An unexpected behaviour was found when the phenyl of **9** was replaced by the furanyl giving **15**. In the series of isoxazoles, the replacement of a phenyl with furanyl or even better with a 5-chlorofuran-2-yl increases the COX-1 selectivity. Instead, the triazole **15** becomes a weak COX-2 inhibitor (40% inhibition at 50 μM). NO_2 of **9** replaced by SCH_3 provides **10** that has a little COX-2 inhibitory activity (14% inhibition at 50 μM), both compounds are not active on COX-1. In our previous investigations, the methoxy was found to be a "*key group*" in the interaction with COX-1 active site [11]. In fact, the *para*-methoxyphenyl ring of a pyrazole derivative (**MPA 14**, Fig. 7) is oriented toward the apex of the COX-1 active site and forms hydrophobic interactions with amino acid residues Phe 518, Met 522, and Ile 523, whereas its methoxy substituent lies within van der Waals contact range of the side chains of Phe 381, Leu 384, Tyr 385, and Trp 387. Notably, the oxygen atom of the *para*-methoxy group forms two contact points to the Trp 387 side chain. Trp 387 is located at the top of the COX-1 active site near the catalytic Tyr 385 residue and has been shown to be critical for the proper positioning of arachidonic acid within the active site to yield the cyclooxygenase product, prostaglandin G_2.

A number of others COX-1 selective inhibitors such as **mofezolac**, **SC-560** (Fig. 6) and **FK881** (Fig. 1) have this group in their chemical structure and in all cases the corresponding molecules are

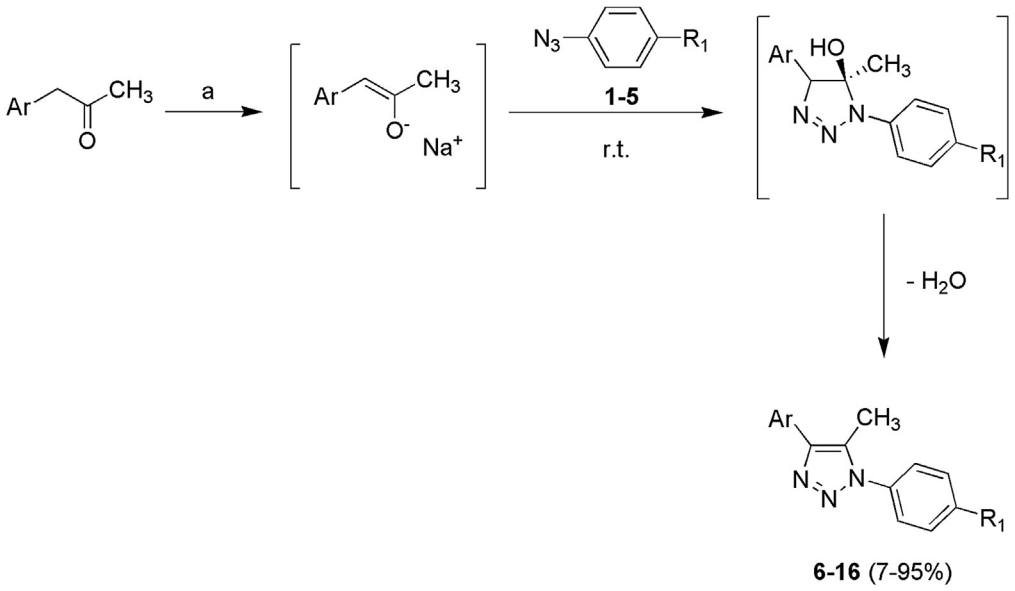

Scheme 2. Reagents and conditions: (a) NaH, THF, 0 °C.

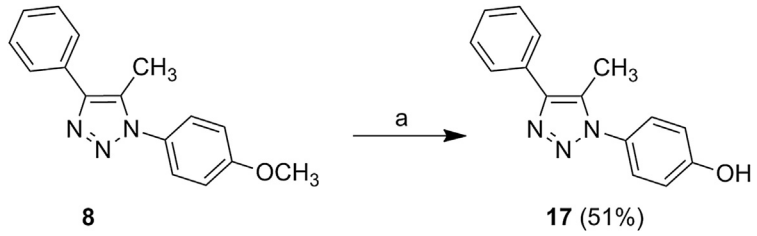

8 **17** (51%)

Scheme 3. Reagents and conditions: (a) BBr_3, dry CH_2Cl_2, r.t.

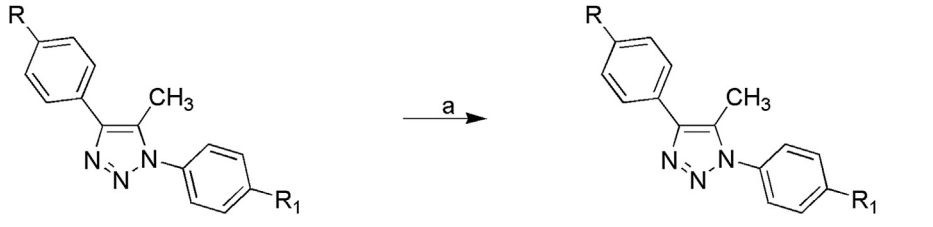

9: R = H, $R_1 = NO_2$
11: R = NO_2, $R_1 = OCH_3$

18: R = H, $R_1 = NH_2$ (58%)
19: R = NH_2, $R_1 = OCH_3$ (30%)

Scheme 4. Reagents and conditions: (a) $SnCl_2$/HCl, EtOH, reflux, 4 h.

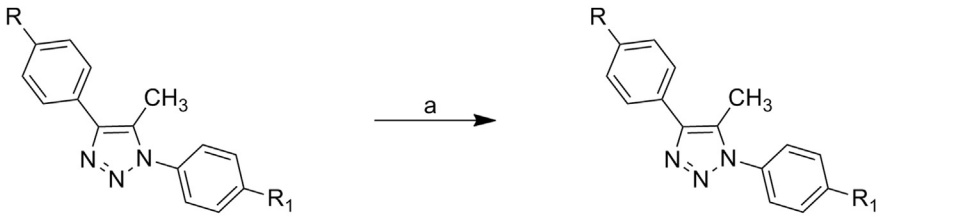

12: R = H, $R_1 = SCH_3$
14: R = SCH_3, $R_1 = OCH_3$

20: R = H, $R_1 = SO_2CH_3$ (42%)
21: R = SO_2CH_3, $R_1 = OCH_3$ (80%)

Scheme 5. Reagents and conditions: (a) *m*CPBA, dry CH_2Cl_2.

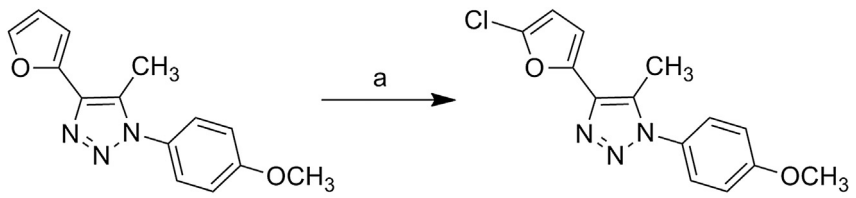

14 **22** (45%)

Scheme 6. Reagents and conditions: (a) *N*-Chlorosuccinimide, dry DMF, 0 °C.

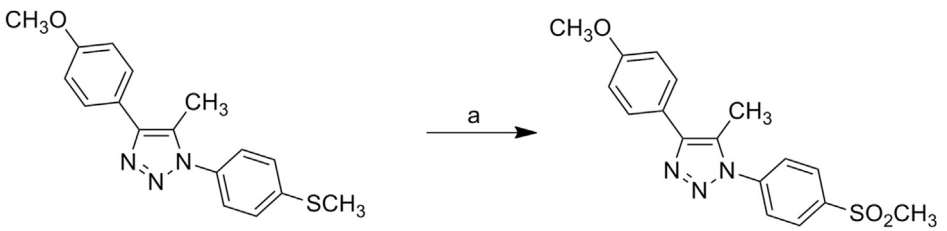

16 **23** (60%)

Scheme 7. Reagents and conditions: (a) *m*CPBA, dry CH_2Cl_2.

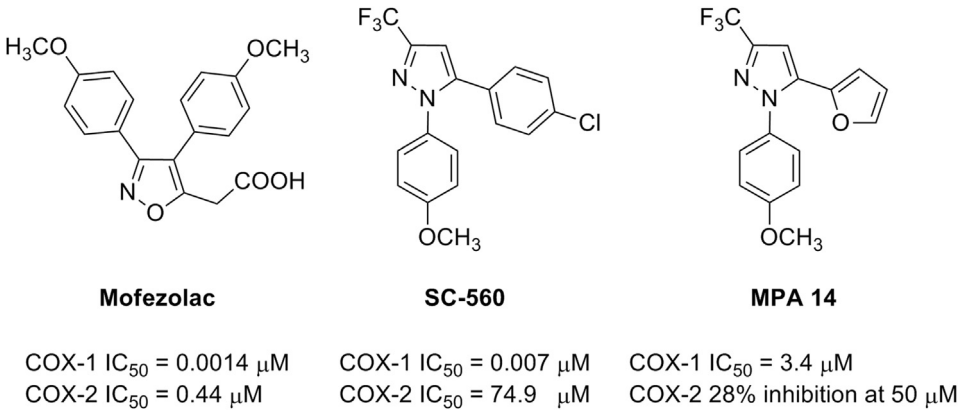

Fig. 6. Mofezolac, SC-560 and **MPA 14** chemical structures and their respective COXs IC_{50} values.

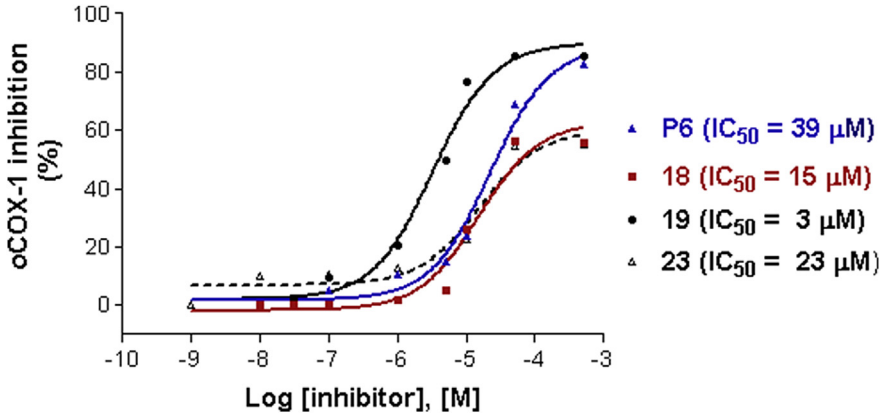

Fig. 7. Concentration-response curves for the inhibition of COX-1 activity by **P6** (▲; IC_{50} = 39 ± 2.4 μM), **18** (■; IC_{50} = 15 ± 4.91 μM), **19** (●; IC_{50} = 3 ± 0.1 μM) **23** (△; IC_{50} = 23 ± 2.4 μM) obtained by a colorimetric COX (ovine) assay kit. IC_{50} values represent the mean ± SEM of three separate experiments.

potent and selective COX-1 inhibitors.

An OCH_3 in the *para* position of the triazole N_1-phenyl of **8**, inhibits the 26 and 35% (at 50 μM) of the catalytic activity of COX-1 and COX-2, respectively. In the series of the 1,2,3-triazoles the OCH_3 presence does not heavily affect the COXs activity and does not determine COX-1 selectivity. The demethylation of **8** ($R_1 = OCH_3$) to **17** (R_1 = OH), determines a complete loss of COX-1 inhibition, a residual COX-2 inhibition is observed (26% inhibition at 50 μM). The inactivity is also found when the C_4-phenyl ring of **8** is substituted with a furan ring (**14**), whereas the introduction of a chlorine on the furyl (**22**) confers approximately a doubling of the inhibitory activity which increases to 45% at 50 μM. Compounds **20** and **21** have been prepared to verify if also in the class of 1,2,3-triazole derivatives the SO_2Me, typical pharmacophore feature of COX-2 inhibitors, at the *para*-position of one of the aryl ring, confers COX-2 selectivity [42]. It is known that SO_2CH_3 is present in most of the Coxibs and is allocated in the COX-2 site pocket not accessible in COX-1 for the presence on the entrance of Ile 523. In our case the methylsulfamoyl substituent is found to be detrimental for COX-2 selectivity (**20**). Unexpectedly, it confers a slight selectivity for COX-1 in **21** (20% inhibition at 50 μM). It seems that the low COX-1 inhibitory activity of **8**, **11**, **13**, and **20** should not be related to the electronic density and/or steric hindrance of the R_1 group (OCH_3) linked to the N_1-triazole. The high COX-1 inhibitory potency of **23** seems due to a synergic effect of OCH_3 and SO_2CH_3 groups, particularly linked to their position in the molecule. Compound **21**, bearing the same groups of its regioisomer **23**, is almost inactive.

The NH_2 group is determinant in the interaction with COX-1 active site. The corresonding isoxazole bearing the NH_2 (**MPA 4** and **MPA 35MPA35**, Table 1), forms strong H-bond with COX-1 Ser 530, which adopts a “down” position during the flexible docking simulation. It does not matter if the NH_2 is bound to the C_5-isoxazole (**MPA 4MPA4**, Table 1) or to the phenyl at C_4-isoxazole (**MPA 35**, Table 1). In fact, compounds **18** (MPA 73) and **19** (MPA 317) bearing the NH_2 are endowed with COX-1 inhibitory activity and selectivity as also predicted by the Volsurf plus model.

The three triazole-nitrogen atoms do not seem to play a significant role, it is not recognized as for the isoxazole ring [12]. *In silico* investigations have shown that the first interactions are H-bonding formation between the nitrogen and oxygen of the isoxazole and COX-1 Tyr 355 [located at the COX entrance, together with Arg 120 and Glu 524 separate the membrane-binding domain (lobby) and the core of the catalitic domain] that during energetic stabilization, a rearrangement of the inhibitor in the active site ultimately results in a stable complex with Ser 530 residue, positioned in the middle of the long hydrophobic channel forming the COXs active site. In particular, a final and stable H-bonding is formed between the furanyl-oxygen atom and the Ser 530-hydroxyl of the COX-1 (Ser 530 is the amino acid acetylated by aspirin during the interaction of acetyl salycilic acid and COXs). Such a positioning of **P6** and its analogues in the COX-1 active site is one of the reasons of their inhibitory potency and selectivity. Based on the COXs inhibition data (Table 2), the 1,2,3-triazole moiety is not able to establish productive interactions, as it is the case of **FK881**, a 1,2,4,-triazole.

By considering the percentage inhibition of COXs by the novel

triazoles, even when in the molecule is present a furyl, it seems that the triazole as core ring is not able to form H-bonds similar to the isoxazole.

Most depends upon molecule volume, electronic and steric features of the substituents present on one or both the aryls linked to the triazole. It seems that is also important for a specific substituent the which aryl is bonded. One aryl is linked to triazole-N_1, whereas the second to the triazole-C_4.

In particular, the presence on N_1-aryl of R_1 = Cl, F, OH, NO_2 or SCH_3 (Scheme 2 and 3, Table 2) renders the molecule unable to inhibit COX-1.

A *p*-OCH_3 on the same N_1-aryl allows the compounds to inhibit COX-1, also depending on the substitution on C_4-aryl. If such a substitution is NO_2, *p*-OCH_3 or *p*-SO_2CH_3 there is a recovery of COX-1 mediated catalysis inhibition. The less hindered furanyl gives compounds still not **14** or poor active **15** endowed with a fair COX-2 inhibition (40% at 50 μM). When the chloro-furanyl is present in the molecule (**22**) a COX-1 inhibition (45% at 50 μM) is observed. Once again the exchange chlorine–hydrogen replacement is detrimental for the potency and selectivity of COX inhibitors [22].

A selective and potent COX-1 inhibitions (Table 1, Fig. 7) were instead obtained when on the *para*-position of N_1-aryl there is SO_2CH_3 and the C_4-aryl is an anisole (**23**), or even better when R_1 is OCH_3 on N_1-phenyl and to the triazole-C_4 is an aniline (**19**), or R_1 of the N_1-phenyl is a NH_2 and C_4-aryl is phenyl (**18**). In fact, the three COX-1 IC_{50} values are 23, 3 and 15 μM, respectively.

Antiproliferative activity of compound **18** and **19** was also measured in MCF-7 human breast adenocarcinoma MCF-7 and SKOV-3 cell lines. No cytotoxic effect was observed [43].

3. Conclusion

A novel set of 1,2,3-triazoles with a variety of chemical groups with different electronic properties, size and shape were projected to test the effect of replacing the isoxazole, pyrazole and 1,2,4-triazole by the triazole as a core ring in diarylheterocycles COXs inhibitors. The adopted strategy also involved a pharmacometric molecular modeling to project active derivatives. Suitable synthetic strategies were developed to obtain the designed compounds, prepared in fair to good yields. Then, the novel 1,2,3-triazoles were evaluated for their capability to inhibit COXs catalytic activity.

The pharmacometric predictive model was built by using as a training set a number of isoxazoles of known COXs inhibitory activity. Experiments confirmed the prediction power of the model developed by using Volsurf plus. It was found that compounds bearing a NH_2 group would be particulary potent and selective COX-1 inhibitor. In fact, **18** and **19** are the most potent and selective COX-1 inhibitors with IC_{50} values of 15 and 3 μM, respectively. Another interesting and unexpected result derived from the COXs inhibitory activity and COX-1 selectivity of **23** bearing the SO_2CH_3 group, the classical "key group" known to achieve COX-2 selectivity. It inhibited only the COX-1 (IC_{50} of 23 μM) leaving unchanged the COX-2 catalytic activity.

In order to improve our knowledge on selective COXs inhibition (particularly COX-1 selective inhibition), investigations of inhibitor-protein interactions by pharmacometric modeling/X-ray/NMR/ESR measurements will be the subsequent step.

4. Experimental

4.1. Chemistry

4.1.1. General methods

Melting points taken on Electrothermal apparatus were uncorrected. ^{1}H NMR and ^{13}C NMR spectra were recorded on 300 MHz on a Varian Mercury-VX Spectrometer and chemical shifts are reported in parts per million (δ). ^{19}F NMR spectra were recorded by using $CFCl_3$ as internal standard. Absolute values of the coupling constant are reported. FT-IR spectra were recorded on a Perkin–Elmer 681 spectrometer. Thin-layer chromatography (TLC) was performed on silica gel sheets with fluorescent indicator, the spots on the TLC were observed under ultraviolet light. Chromatography was conducted by using silica gel 60 with a particle size distribution 40–63 μm and 230-400 ASTM. GC–MS analyses were performed on an HP 5995C model and elemental analyses on an Elemental Analyzer 1106-Carlo Erba-instrument. ESI-MS analyses were performed on an Agilent 1100 LC/MSD trap system VL. All synthesized compounds were analyzed by HPLC analysis performed on an Agilent 1260 Infinity instrument equipped with a 1260 DAD VL + detector, and their purity is higher than 95%. Structure elucidation of the 1,4-diaryl-1,2,3-triazoles was performed by 2D NOESY spectra recorded on a Bruker 600 MHz: as mentioned above, with careful attention to the spatial connectivity revealed by the correlation between diagnostic methyl and proton signals of both aromatic rings. The 2D data of compound **8** and **14** (Figs. 8 and 9) were then used to definitively attribute chemical structures to 1,4-diaryl-1,2,3-triazoles **6**–**23**.

4.1.2. General procedure for the preparation of arylazides ***1***–***5*** *[41]*

To a solution of moist NaN_3 (6mmol/300 μL water) in *t*-BuOH (2 mL) the opportune arylazide, dissolved in *t*-BuOH (3 mL), was added dropwise. The reaction mixture was stirred overnight at r.t. The reaction products were extracted with EtOAc. The organic phase was dried over anhydrous Na_2SO_4 and then the solvent was evaporated under reduced pressure. The product was isolated by column chromatography (silica gel Hexane/EtOAc 8:2). All spectroscopic data are in accordance with published findings [44].

4.1.3. General procedure for the preparation of triazoles ***6***–***13***

To a stirring suspension of NaH (1 eq.) in THF (3 mL) kept at 0 °C a solution of the proper ketone (0.5 eq.) in THF (3 mL) was added dropwise (Scheme 2, Table 2). The reaction mixture was stirred at 0 °C for 1 h. Then, a solution of the opportune arylazide (0.5 eq.) in THF (3 mL) was added dropwise and the reaction mixture was stirred at r.t. till the disappearance of the arylazide (18h). The reaction mixture was quenched by adding aqueous NH_4Cl, and the reaction product was extracted three times with ethyl acetate. The combined organic phases were dried over anhydrous Na_2SO_4 and then evaporated under vacuum.

*4.1.3.1. 1-(4-Chlorophenyl)-5-methyl-4-phenyl-1H-1,2,3-triazole (**6**).* The product was isolated as a yellow solid (14% yield) by column chromatography (silica gel, hexane/EtOAc = 7:3); mp: 138–140 °C; ^{1}H NMR (300 MHz, $CDCl_3$): δ 7.77–7.74 (m, 2H, aromatic protons), 7.56–7.53 (m, 2H, aromatic protons), 7.51–7.36 (m, 5H, aromatic protons), 2.48 ppm (s, 3H, *CH*$_3$). ^{13}C NMR (75 MHz, $CDCl_3$): δ 145.3, 135.8, 135.1, 131.4, 130.0, 129.8, 129.0, 128.2, 127.5, 126.7, 10.5. FT-IR (KBr): 3057, 1503, 1459, 1445, 1406, 1384, 1253, 1120, 1095, 1072, 1007, 838, 768, 717, 695 cm^{-1}; GC–MS (70 eV) *m/z* (rel.int.): 271 [(M^+ + 2), 1], 269 (M^+, 4), 241 (100), 206 (63), 191 (5), 178 (8), 165 (85), 115 (15), 103 (65), 89 (15), 77 (27).

*4.1.3.2. 1-(4-Fluorophenyl)-5-methyl-4-phenyl-1H-1,2,3-triazole (**7**).* The product was isolated as a yellow oil (20% yield) by column chromatography (silica gel, hexane/EtOAc = 9:1). ^{1}H NMR (300 MHz, $CDCl_3$): δ 7.78–7.75 (m, 2H, aromatic protons), 7.52–7.46 (m, 4H, aromatic protons), 7.41–7.35 (m, 2H, aromatic protons), 7.30–7.22 (m, 2H, aromatic protons), 2.46 (s, 3H, *CH*$_3$). ^{13}C NMR (75 MHz, $CDCl_3$): δ 163.2 (d, $^1J_{19F-13C}$ = 250 Hz), 145.1, 132.7 (d, $^3J_{19F-13C}$ = 7.9 Hz), 131.5, 130.0, 129.0, 128.1, 127.6, 127.4, 116.9 (d,

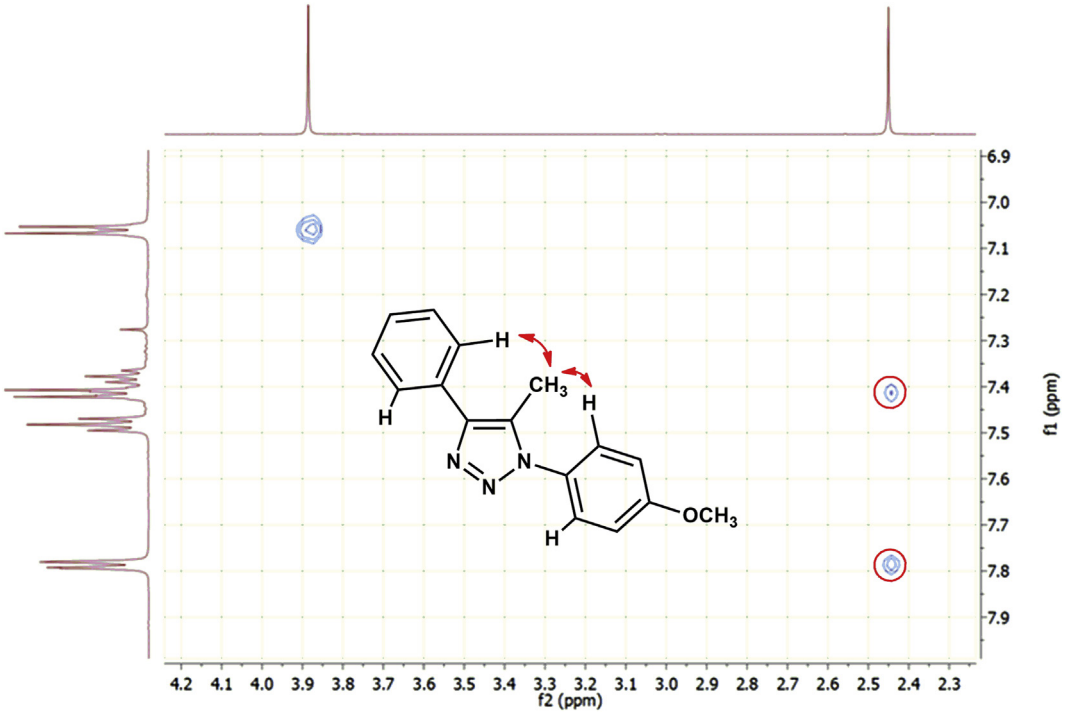

Fig. 8. 2D NOESY experiment for compound **8**.

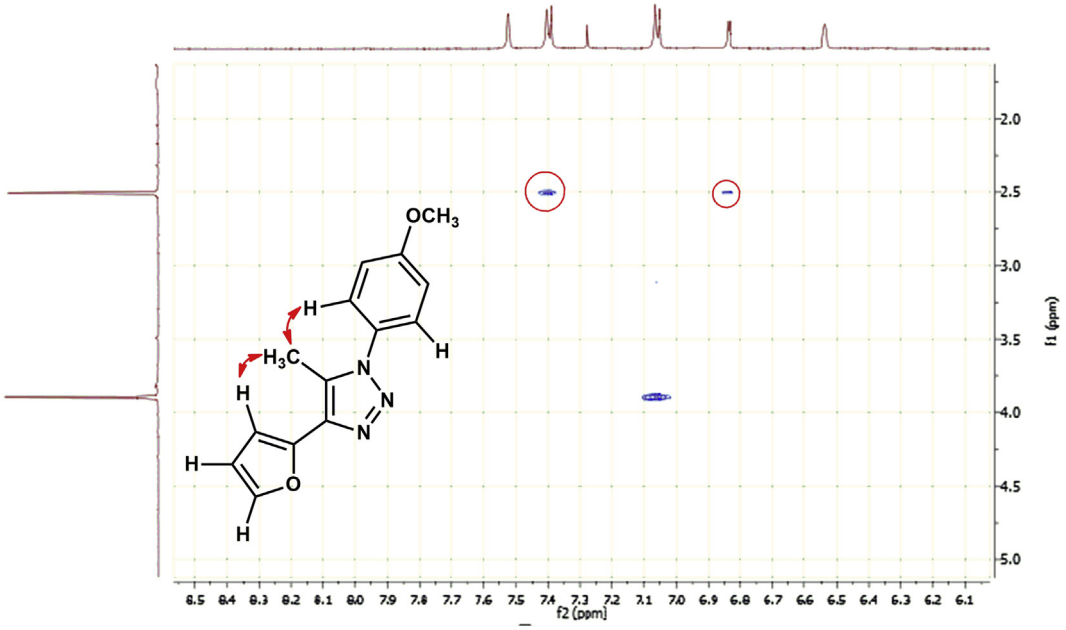

Fig. 9. 2D NOESY experiment of compound **14**.

$^{2}J_{19F-13C}$ = 23 Hz), 10.4. ^{19}F NMR (376 MHz, $CDCl_3$): δ = - 111.37. FT-IR (KBr): 3051, 1604, 1518, 1444, 1415, 1383, 1236, 1157, 1115, 1091, 841, 820, 769, 720, 698 cm^{-1}. GC–MS (70 eV) *m/z* (rel. int.): 253 (M^+, 3), 225 (100), 210 (4), 196 (4), 183 (85), 148 (18), 122 (8), 103 (41).

*4.1.3.3. 1-(4-Methoxyphenyl)-5-methyl-4-phenyl-1H-1,2,3-triazole (**8**).* The product was isolated as a yellow solid (48% yield) by column chromatography (silica gel, hexane/EtOAc = 9:1); mp: 132.0–135.0 °C. ^{1}H NMR (300 MHz, $CDCl_3$): δ 7.79–7.78 (m, 2H, aromatic protons), 7.76–7.34 (m, 5H, aromatic protons), 7.08–7.03 (m, 2H, aromatic protons), 3.89 (s, 3H, OCH_3), 2.45 (s, 3H, CH_3). ^{13}C NMR (75 MHz, $CDCl_3$): δ 160.5, 144.8, 131.7, 130.2, 129.5, 129.0, 128.0, 127.4, 126.9, 114.8, 55.9, 10.4. FT-IR (KBr): 3053, 2967, 2932, 1610, 1519, 1444, 1307, 1257, 1020, 841, 775, 697 cm^{-1}. GC–MS (70 eV) *m/z* (rel. int.): 265 (M^+, 2), 237 (100), 222 (53), 207 (5), 194 (66), 165 (12), 152 (22), 103 (20). The unambiguous structure elucidation of this product was achieved by 2D NOESY spectrum: in, the diagnostic cross-peaks between the methyl protons (2.4 ppm) and both the aromatic proton signals (7.4 and 7.8 ppm, respectively) were evidenced (Fig. 8).

*4.1.3.4. 5-Methyl-1-(4-nitrophenyl)-4-phenyl-1H-1,2,3-triazole (**9**) [45].* The product was isolated as a yellow solid (70% yield) by column chromatography (silica gel, hexane/EtOAc = 7:3); mp: 197.4–200.2 °C. ^{1}H NMR (300 MHz, $CDCl_3$): δ 8.49–8.44 (m, 2H, aromatic protons); 7.81–7.75 (m, 4H, aromatic protons); 7.53–7.48 (m, 2H, aromatic protons); 7.43–7.39 (m, 1H, aromatic proton); 2.58 (s, 3H, CH_3). ^{13}C NMR (75 MHz, $CDCl_3$): δ 148.0, 146.2, 141.4, 130.9, 129.7, 129.1, 128.5, 127.6, 125.6, 125.4, 10.8. FT-IR (KBr): 3093, 2922, 1615, 1599, 1523, 1503, 1346, 1268, 863, 855 cm^{-1}. GC–MS (70 eV) *m/z* (rel. int.): 280 (M^+, 6), 252 (44), 206 (100), 191 (14), 178 (19), 165 (43), 115 (15), 103 (37).

*4.1.3.5. 5-Methyl-1-[4-(methylthio)phenyl]-4-phenyl-1H-1,2,3-triazole (**10**).* The product was isolated as an orange solid (35% yield) by column chromatography (silica gel, hexane/EtOAc = 7:3); mp: 149.1–153.0 °C. ^{1}H NMR (300 MHz, $CDCl_3$): δ 7.79–7.76 (m, 2H, aromatic protons); 7.51–7.40 (m, 7H, aromatic protons); 2.55 (s, 3H, SCH_3); 2.47 (s, 3H, CH_3). ^{13}C NMR (75 MHz, $CDCl_3$): δ 145.1, 141.2, 133.4, 131.6, 129.9, 129.0, 128.0, 127.5, 127.0, 125.8, 15.8, 10.5. FT-IR (KBr): 3053, 2919, 2851, 1610, 1504, 1438, 1402, 1384, 1258, 1094, 1074, 820, 837, 771, 716, 698 cm^{-1}. GC–MS (70 eV) *m/z* (rel. int.): 281 (M^+, 4), 253 (68), 238 (100), 220 (14), 206 (99), 178 (15), 165 (48), 150 (9), 130 (8), 115 (11), 103 (44).

*4.1.3.6. 1-(4-Methoxyphenyl)-5-methyl-4-(4-nitrophenyl)-1H-1,2,3-triazole (**11**).* The product was isolated as a brown solid (95% yield) by column chromatography (silica gel, hexane/EtOAc = 7:3); mp: 225–230 °C. ^{1}H NMR (300 MHz, $CDCl_3$): δ 8.36–8.33 (m, 2H, aromatic protons); 8.01–7.97 (m, 2H, aromatic protons); 7.43–7.40 (m, 2H, aromatic protons), 7.09–7.07 (m, 2H, aromatic protons); 3.90 (s, 3H, OCH_3); 2.52 (s, 3H, CH_3). ^{13}C NMR (75 MHz, DMSO-d_6): δ 160.8, 147.2, 142.6, 138.3, 131.6, 128.9, 127.5, 127.1, 124.4, 115.0, 55.9, 10.7. ESI-MS: *m/z* (%): $C_{16}H_{14}N_4O_3$, 333 $(M + Na)^+$. FT-IR (KBr): 3432, 2965, 2921, 1601, 1564, 1519,1503, 1488, 1337, 1254, 1169, 835, 717 cm^{-1}.

*4.1.3.7. 1-(4-Methoxyphenyl)-5-methyl-4-[4-(methylthio)phenyl]-1H-1,2,3-triazole (**12**).* The product was isolated as a white solid (50% yield) by column chromatography (silica gel, hexane/EtOAc = 7:3); mp: 184–186 °C; ^{1}H NMR (300 MHz, $CDCl_3$): δ 7.72–7.68 (m, 2H, aromatic protons); 7.42–7.26 (m, 4H, aromatic protons); 7.25–7.04 (m, 2H, aromatic protons); 3.89 (s, 3H, OCH_3); 2.53 (s, 3H, SCH_3); 2.43 (s, 3H, CH_3). ^{13}C NMR (75 MHz, $CDCl_3$): δ 159.6, 145.7, 141.2, 140.7129.1, 128.7, 128.7125.6, 123.3, 114.3, 55.3, 44.5, 10.5. FT-IR (KBr): 2960, 2923, 2851, 1519, 1304, 1259, 1149,1092, 1016, 838, 803 cm^{-1}. GC–MS (70 eV) *m/z* (rel. int.): 311 (M^+,8), 283 (100), 268 (79), 253 (9), 240 (31), 221 (14), 207 (7), 195 (12), 165 (7), 152 (21),134 (14), 120 (9), 103 (6), 92 (11), 77 (12), 64 (8).

*4.1.3.8. 1,4-Bis-(4-methoxyphenyl)-5methyl-1H-1,2,3-triazole (**13**).* The product was isolated as a brown solid (41% yield) by column chromatography (silica gel, hexane/EtOAc = 6:4); mp: 162–163 °C; ^{1}H NMR (300 MHz, $CDCl_3$): δ 7.74–7.64 (m, 2H, aromatic protons); 7.46–7.37 (m, 2H, aromatic protons); 7.29–7.20 (m, 4H, aromatic protons); 3.88 (s, 3H, OCH_3); 3.85 (s, 3H, OCH_3); 2.41 (s, 3H, CH_3). ^{13}C NMR (75 MHz, $CDCl_3$): δ 160.5, 159.5, 144.7, 129.5, 128.7, 126.9, 124.3, 114.8, 114.4, 56.0, 55.7, 55.4, 10.4. FT-IR (KBr): 2955, 2934, 2837, 1617, 1520, 1467, 1439, 1247, 1176, 1117, 1049, 1024, 834 cm^{-1}. GC–MS (70 eV) *m/z* (rel. int.): 295 (15), 267 (100), 266 (95), 224 (25), 211 (20), 92 (22), 77 (25).

*4.1.3.9. 4-(Furan-2-yl)-1-(4-methoxyphenyl)-5-methyl-1h-1,2,3-triazole (**14**).* The product was isolated as a brown oil (45% yield) by column chromatography (silica gel, hexane/EtOAc = 7:3); ^{1}H NMR (300 MHz, $CDCl_3$): δ 7.52–7.51 (m, 1H, furyl proton); 7.41–7.36 (m, 2H, aromatic protons); 7.07–7.02 (m, 2H, aromatic protons); 6.83–6.82 (m, 1H, furyl proton); 6.53–6.51 (m, 1H, furyl proton); 3.88 (s, 3H, OCH_3); 2.49 (s, 3H, CH_3). ^{13}C NMR (75 MHz, $CDCl_3$): δ 160.6, 147.3, 142.2, 137.9, 130.0, 129.1, 126.9, 114.9, 111.5, 106.9, 55.9, 9.8. FT-IR (KBr): 3130, 2919, 1610, 1518, 1463, 1384, 1302, 1255, 1020, 838 cm^{-1}. GC–MS (70 eV) *m/z* (rel. int.): 255 (M^+,94) 227 (66), 212 (65), 198 (52), 184 (100), 167 (27), 115 (52), 92 (54), 77 (77), 64 (43). The unambiguous structure elucidation of this product was achieved by 2D NMR spectroscopy (Fig. 9), as evidenced by the diagnostic cross-peaks between the methyl protons (2.49 ppm) and the proton signals of both the aromatic rings (7.40 and 6.84 ppm, respectively).

*4.1.3.10. 4-(Furan-2-yl)-5-methyl-1-(4-nitrophenyl)-1h-1,2,3-triazole (**15**).* The product was isolated as a yellow oil (7% yield) by column chromatography (silica gel, HEXANE/EtOAc 7:3); ^{1}H NMR (300 MHz, $CDCl_3$): δ 8.47–8.43 (m, 2H, aromatic protons); 7.79–7.74 (m, 2H, aromatic protons); 7.55–7.54 (m, 1H, furyl proton); 6.90–6.88 (m, 1H, furyl proton); 6.56–6.55 (m, 1H, furyl proton); 2.64 (s, 3H, CH_3). ESI-MS: *m/z* (%): $C_{13}H_{10}N_4O_3$, 293 $(M + Na)^+$.

*4.1.3.11. 4-(4-Methoxyphenyl)-5-methyl-1-[4-(methylthio)phenyl]-1H-1,2,3-triazole (**16**).* The product was isolated as a white solid (33% yield) by crystallization from hexane/$CHCl_3$); mp: 184.9–185 °C; ^{1}H NMR (300 MHz, $CDCl_3$): δ 7.70–7.68 (m, 2H, aromatic protons); 7.44–7.37 (m, 4H, aromatic protons); 7.03–6.99 (m, 2H, aromatic protons); 3.86 (s, 3H, OCH_3); 2.55 (s, 3H, SCH_3); 2.44 (s, 3H, CH_3). ^{13}C NMR (75 MHz, $CDCl_3$): δ 159.5, 144.9, 141.1, 133.5, 129.2, 128.7, 126.9, 125.7, 124.2, 114.4, 55.6, 55.5, 10.5. FT-IR (KBr): 2920, 2834, 1640, 1614, 1510, 1384, 1247, 1384, 1247, 1177, 1026, 832, 528 cm^{-1}. GC–MS (70 eV) *m/z* (rel. int.): 311 (20), 283 (37), 268 (48), 236 (100), 152 (12), 77 (11). HRMS (ESI) Calcd for $C_{17}H_{18}N_3OS$: 312,1171 $[M+H]^+$, Found: 312,1156 $[M+H]^+$.

*4.1.3.12. Synthesis of 4-(5-methyl-4-phenyl-1H-1,2,3-triazol-1-yl) phenol (**17**) [44].* To a stirred solution of 1-(4-methoxyphenyl)-5-methyl-4-phenyl-1*H*-1,2,3-triazole (**8**) (83 mg, 0.31 mmol) in dry CH_2Cl_2 (5 mL) kept at −50 °C, BBr_3 (1 mL, 0.31 mmol) was added. The stirred reaction mixture was kept at room temperature for 1 h. Then, $NaHCO_3$ (5 mL) was added and the aqueous phase extracted three times with EtOAc. The combined organic extracts were dried over anhydrous Na_2SO_4 and the solvent was removed under reduced pressure. The product was isolated as a white solid (51% yield) by column chromatography (silica gel, hexane/EtOAc = 1:1); mp: 200–203 °C. ^{1}H NMR (300 MHz, $CDCl_3$): δ 10.04 (OH, exchange with D_2O); 7.75–7.74 (m, 2H, aromatic protons); 7.72–7.48 (m, 2H, aromatic protons); 7.47–7.37 (m, 3H, aromatic protons), 6.97–6.94 (m, 2H, aromatic protons); 2.38 (s, 3H, CH_3). ^{13}C NMR (75 MHz, DMSO-d_6): δ 159.1, 143.8, 132.1, 131.1, 129.5, 128.2, 128.1, 127.5, 127.3, 116.6, 10.5. ESI-MS: *m/z* (%): $C_{15}H_{13}N_3O$, 274 $(M + Na)^+$. FT-IR (KBr): 3445 (broad), 2923, 2852, 1637, 1513, 1494, 1456, 1076, 843, 780 cm^{-1}.

4.1.4. General procedure for the synthesis of 4-(5-methyl-4-phenyl-1H-1,2,3-triazol-1-yl)benzenamine (18) and 4-[1-(4-methoxyphenyl)-5-methyl-1H-1,2,3-triazole-4-yl]benzenamine (19)

To a stirred solution of stannous chloride (0.72 mmol) in HCl 37% (1 mL) was added dropwise 5-methyl-1-(4-nitrophenyl)-4-phenyl-1*H*-1,2,3-triazole **(9)** (0.18 mmol) or 1-(4-methoxyphenyl)-5-methyl-4-(4-nitrophenyl)-1*H*-1,2,3-triazole **(11)** (0.18 mmol) dissolved in absolute EtOH (12 mL). The stirred reaction mixture was kept at 80 °C for 4 h. Then 10% NaOH (10 mL) was added to the reaction mixture till pH = 12, and the aqueous phase was extracted

three times with EtOAc. The combined organic extracts were dried over anhydrous Na_2SO_4 and the solvent removed under reduced pressure.

*4.1.4.1. 4-(5-Methyl-4-phenyl-1H-1,2,3-triazol-1-yl)benzenamine (**18**) [45].* The product was isolated as a brown solid (58% yield) by column chromatography (silica gel, petroleum ether/EtOAc = 8:2); mp: 181–184 °C. ^{1}H NMR (300 MHz, $CDCl_3$): δ 7.79–7.76 (m, 2H, aromatic protons); 7.51–7.31 (m, 3H, aromatic protons); 7.28–7.23 (m, 2H, aromatic protons), 6.91–6.78 (m, 2H, aromatic protons); 4.95 (NH_2, exchange with D_2O); 2.44 (s, 3H, CH_3). ^{13}C NMR (75 MHz, $CDCl_3$): δ 147.9, 144.6, 131.9, 130.1, 128.9, 127.9, 127.3, 127.3, 126.9, 115.3, 10.4. FT-IR (KBr): 3419, 3347, 3237, 1645,1607, 1521, 1492, 1442, 1308, 1257, 1170, 1134, 1073, 830, 771, 720, 704, 697 cm^{-1}. GC–MS (70 eV) *m/z* (rel. int.): 250 (2), 222 (100), 204 (75), 180 (31), 145 (12), 118 (9), 103 (15), 89 (6), 65 (15). HRMS (ESI) Calcd for $C_{15}H_{15}N_4$: 251.1291 $[M+H]^+$, Found: 251.1292 $[M+H]^+$.

*4.1.4.2. 4-[1-(4-Methoxyphenyl)-5-methyl-1H-1,2,3-triazole-4-yl] benzenamine (**19**).* The product was isolated as a brown solid (30% yield) by column chromatography (silica gel, hexane/EtOAc = 3:7); mp: 165–166 °C; ^{1}H NMR (300 MHz, $CDCl_3$): δ 7.58–7.55 (m, 2H, aromatic protons); 7.42–7.39 (m, 2H, aromatic protons); 7.06–7.03 (m, 2H, aromatic protons), 6.80–6.77 (m, 2H, aromatic protons); 3.88 (s, 3H, OCH_3); 3.48 (NH_2, exchange with D_2O); 2.40 (s, 3H, CH_3). ^{13}C NMR (75 MHz, $CDCl_3$): δ 160.4, 146.3, 145.1, 129.7, 129.0, 128.6, 126.9, 122.1, 115.0, 114.8, 55.8, 22.9. ESI-MS: *m/z* (%): $C_{16}H_{16}N_4O$, 303 $(M + Na)^+$. FT-IR (KBr): 2956, 2918, 2850, 2581, 1610, 1513, 1463, 1254, 1096, 1027, 833 cm^{-1}. HRMS (ESI) Calcd for $C_{16}H_{17}N_4O$: 281,1402 $[M+H]^+$, Found: 281,1395 $[M+H]^+$.

4.1.5. General procedure for the synthesis of 5-methyl-1-[4-(methylsulfonyl)phenyl]-4-phenyl-1H-1,2,3-triazole (20) and 1-(4-methoxyphenyl)-5-methyl-4-[4-(methylsulfonyl)phenyl]-1H-1,2,3-triazole (21) and 4-(4-methoxyphenyl)-5-methyl-1-(4-methylsulfonylphenyl)-1H-1,2,3-triazole (23)

m-Chloroperoxybenzoic acid (0.26 mmol) was added to an ice-cold stirred solution of 5-methyl-1-[4-(methylthio)phenyl]-4-phenyl-1*H*-1,2,3-triazole (**10**) (0.13 mmol) or 1-(4-methoxyphenyl)-5-methyl-4-[4-(methylthio)phenyl]-1*H*-1,2,3-triazole (**12**) or 4-(4-methoxyphenyl)-5-methyl-1-[4-(methylthio) phenyl]-1*H*-1,2,3-triazole (**16**) in dry CH_2Cl_2 (5 mL). The reaction mixture was stirred and slowly allowed to reach room temperature. Then, the reaction mixture was stirred for 1 h. Water (5 mL) was added and the aqueous phase extracted three times with EtOAc. The combined organic extracts were dried over anhydrous Na_2SO_4 and the solvent removed under reduced pressure.

*4.1.5.1. 5-Methyl-1-[4-(methylsulfonyl)phenyl]-4-phenyl-1H-1,2,3-triazole (**20**).* The product was isolated as a white solid (42% yield) by column chromatography (silica gel, hexane/EtOAc = 3:7); mp: 231–234 °C. ^{1}H NMR (300 MHz, $CDCl_3$): δ 8.18–8.16 (m, 2H, aromatic protons); 7.81–7.52 (m, 4H, aromatic protons); 7.50–7.47 (m, 2H, aromatic protons), 7.43–7.40 (m, 1H, aromatic protons); 3.14 (s, 3H, SO_2CH_3); 2.56 (s, 3H, CH_3). ^{13}C NMR (75 MHz, $CDCl_3$): δ 146.0, 141.5, 140.8, 131.0, 129.3, 129.1, 128.4, 127.6, 125.9, 44.7, 10.7. FT-IR (KBr): 3025, 3010, 2958, 1505, 1446, 1385, 1300, 1155, 788, 746, 692 cm^{-1}. GC–MS (70 eV) *m/z* (rel. int.): 313 (2), 285 (12), 207 (15), 206 (100), 205 (11), 204 (16), 178 (11), 165 (24), 103 (21).

*4.1.5.2. 1-(4-Methoxyphenyl)-5-methyl-4-[4-(methylsulfonyl) phenyl]-1H-1,2,3-triazole (**21**).* The product was isolated as a white solid (80% yield) by crystallization from hexane/EtOAc; mp: 241–242 °C; ^{1}H NMR (300 MHz, $CDCl_3$): δ 8.07–7.99 (m, 4H, aromatic protons); 7.43–7.40 (m, 2H, aromatic protons); 7.09–7.06 (m, 2H, aromatic protons); 3.90 (s, 3H, OCH_3); 3.10 (s, 3H, SCH_3); 2.50 (s, 3H, CH_3). ^{13}C NMR (75 MHz, $CDCl_3$): δ 160.8, 142.9, 139.4, 137.3, 131.4, 129.0, 128.1, 127.7, 127.0, 115.0, 55.9, 44.7, 10.6. FT-IR (KBr): 3421,2961, 2924, 2852, 2361, 2343, 1734, 1609, 1518, 1458, 1303, 1148, 1091, 1016, 802 cm^{-1}. ESI-MS: *m/z* (%): $C_{17}H_{17}N_3O_3S$, 366 $(M + Na)^+$.

*4.1.5.3. 4-(4-Methoxyphenyl)-5-methyl-1-[4-(methylsulphonyl) phenyl]-1H-1,2,3-triazole (**23**).* The product was isolated as a white solid (60% yield) by column chromatography (silica gel, hexane/EtOAc = 3:7); mp: 240.9–241.5 °C; ^{1}H NMR (300 MHz, $CDCl_3$): δ 8.19–8.15 (m, 2H, aromatic protons); 7.81–7.77 (m, 2H, aromatic protons); 7.71–7.66 (m, 2H, aromatic protons); 7.04–7.00 (m, 2H, aromatic protons); 3.13 (s, 3H, OCH_3); 2.53 (s, 3H, SO_2CH_3); 1.25 (s, 3H, CH_3). ^{13}C NMR (75 MHz, $CDCl_3$): δ 159.6, 145.0, 141.1, 133.5, 129.2, 128.7, 127.0, 125.7, 124.2, 114.4, 55.6, 38.4, 10.5. ESI-MS: *m/z* (%): $C_{16}H_{14}N_4O_3$, 366 $(M + Na)^+$. HRMS (ESI) Calcd for $C_{17}H_{18}N_3O_3S$: 344,1069 $[M+H]^+$, Found: 344,1073 $[M+H]^+$.

*4.1.6. Synthesis of 4-(5-chlorofuran-2-yl)-1-(4-methoxyphenyl)-5-methyl-1H-1,2,3-triazole (**22**)*

A mixture of 4-(furan-2-yl)-1-(4-methoxyphenyl)-5-methyl-1*H*-1,2,3-triazole (**14**) (65 mg, 0.255 nmol) in anhydrous DMF (4 mL) was stirred at 0 °C under inert atmosphere. The reaction mixture was allowed to reach room temperature, then *N*-chlorosuccinimide (36 mg, 0.273 mmol) was added at 10 min intervals partitioned in three times. The reaction mixture was monitored by TLC (silica gel, hexane/EtOAc = 8:2) and stirred until the disappearance of **14** (approximately 5 h). The reaction mixture was quenched by adding H_2O. The reaction product was extracted three times with ethyl acetate. The combined organic phases were dried over anhydrous Na_2SO_4 and the solvent evaporated under vacuum. The product was isolated as a yellow oil (45% yield) by column chromatography (silica gel, hexane/EtOAc = 8:2); ^{1}H NMR (300 MHz, $CDCl_3$): δ 7.40–7.36 (m, 2H, aromatic protons); 7.08–7.04 (m, 2H, aromatic protons); 6.83–6.81 (m, 1H, furyl proton); 6.30–6.29 (m, 1H, furyl proton); 3.89 (s, 3H, OCH_3); 2.48 (s, 3H, CH_3). ^{13}C NMR (75 MHz, $CDCl_3$): δ 160.7, 146.8, 137.0, 136.2, 130.2, 129.0, 126.9, 114.9, 109.0, 108.2, 55.9, 9.8. FT-IR (KBr): 2918, 2850, 2360, 2343, 1703, 1519, 1256, 1216, 836 cm^{-1}. GC–MS (70 eV) *m/z* (rel. int.): 289 (M^+,14), 261 (23), 246 (21), 226 (100), 218 (26), 198 (52), 183 (40), 155 (24), 113 (12), 92 (19), 77 823), 64 (15). HRMS (ESI) Calcd for $C_{14}H_{13}ClN_3O_2$: 290,0696 $[M+H]^+$, Found: 290,0692 $[M+H]^+$.

4.2. Computational methods

4.2.1. VolSurf plus descriptors

The interaction of molecules with biological membranes is mediated by surface properties such as shape, electrostatic forces, H-bonds and hydrophobicity. Therefore, the GRID [17] force field was chosen to characterize potential polar and hydrophobic interaction sites around target molecules by the water (OH_2), the hydrophobic (DRY), and the carbonyl oxygen (O) and amide nitrogen (N1) probe. The information contained in the MIF is transformed into a quantitative scale by calculating the volume or the surface of the interaction contours. The VolSurf plus procedure is as follows: i) in the first step, the 3D molecular field is generated from the interactions of the OH_2, the DRY, O and N1 probe around a target molecule; ii) the second step consists in the calculation of descriptors from the 3D maps obtained in the first step. The molecular descriptors obtained, called VolSurf plus descriptors, refer to molecular size and shape, to hydrophilic and hydrophobic regions and to the balance between them, to molecular diffusion, LogP, LogD, to the "*charge state*" descriptors, to the new 3D pharmacophoric

descriptors and to some descriptors on some rilevant ADME properties. In total VolSurf plus uses 128 descriptors [46–48]; iii) finally, chemometric tools (PCA [49], PLS [50,51]) are used to create relationships of the VolSurf plus descriptor matrix with ADME properties. The scheme of the VolSurf plus programme steps and a detailed definition of Volsurf plus descriptors have recently been reported [52].

4.3. Biology

4.3.1. Cyclooxygenase inhibition studies

The target compounds **6**–**23** were evaluated for their ability to inhibit ovine COX-1/COX-2 enzyme (percent inhibition at 50 μM). Inhibition of the enzyme was determined using a colorimetric COX (ovine) inhibitor screening assay kit (Catalog No. 760111, Cayman Chemicals, Ann Arbor, MI, USA) following the procedure described in the catalog according to the manufacturer's instructions.

COX is a bifunctional enzyme exhibiting both cyclooxygenase and peroxidase activity. The COX component converts arachidonic acid to a hydroperoxide (PGG_2), and the peroxidase component reduces the endoperoxide to the corresponding alcohol (PGH_2), the precursor of PGs, thromboxanes, and prostacyclins. The Colorimetric COX Inhibitor Screening Assay measures the peroxidase component of overall cyclooxygenases activity. The peroxidase activity is assayed colorimetrically by monitoring the appearance of oxidized *N,N,N′,N′*-tetramethyl-*p*-phenylenediamine (TMPD) at 590 nm. **6**–**23** were dissolved in a minimum volume of DMSO to prepare to stock solutions.

4.3.2. Antiproliferative assay

Determination of cell growth was performed using the MTTassay at 48 h. On day 1,30,000 cells/well were seeded into 96-well plates in a volume of 100 μL. On day 2, the various drugs concentration (0.1–100 μM) were added. In all the experiments, the drug solvent (DMSO) was added in each control to evaluate a possible solvent cytotoxicity. After the established incubation time with drugs, MTT (0.5 mg/mL) was added to each well, and after 3 h incubation at 37 °C, the supernatant was removed. The formazan crystals were solubilized using 100 μL of DMSO and the absorbance values at 570 nm was determined on the microplate reader Victor 3 from PerkinElmer Life Sciences.

4.4. Statistical analysis

The IC_{50} values of the compounds reported in Fig. 7 and Table 2 were determined by nonlinear curve fitting using the GraphPad Prism program (GraphPad Prism Software (Windows version), Graph-Pad Software, Inc., San Diego, CA, USA) and are the mean ± SEM from three separate experiments.

Acknowledgements

Thanks are due to Laboratorio di Ricerca per la Diagnostica dei Beni Culturali (University of Bari) and to C.I.N.M.P.I.S. Consortium for NMR facilities. Thanks are due also to (a) Public Research Laboratories Networks of Regione Puglia-APQ Research Programme 'Integrated renewable energy generation from the regional agro-industrial sector. Project Code 01'. (Intervento cofinanziato dall'Accordo di Programma Quadro in materia di Ricerca Scientifica – II Atto Integrativo – PO FESR 2007–2013, Asse I, Linea 1.2-PO FSE 2007–2013 Asse IV "Investiamo nel vostro futuro"); (b) MIUR (Rome e Italy) for Progetti di Ricerca Industriale nell'ambito del Programma Operativo Nazionale R&C 2007e2013 e Project "Reasearch, Application, Innovation, Services in Bioimaging (R.A.I.SE.)" code PON01_03054. The authors would like to thank Dr. Luciana Cicco for her contribution to the synthesis of some of novel target compounds and to Dr. Francesco Cannito and to Consorzio Interuniversitario di Ricerca in Chimica dei Metalli nei Sistemi Biologici (C.I.R.C.M.S.B.) Bari for HR-MS analysis.

Appendix A. Supplementary data

Supplementary data related to this article can be found at http://dx.doi.org/10.1016/j.ejmech.2015.02.049.

References

[1] M.G. Perrone, A. Scilimati, L. Simone, P. Vitale, Selective COX-1 inhibition: a therapeutic target to be reconsidered, Curr. Med. Chem. 17 (2010) 3769–3805.
[2] M.G. Perrone, P. Malerba, J. Uddin, P. Vitale, A. Panella, B.C. Crews, C.K. Daniel, K. Ghebreselasie, M. Nickels, M.N. Tantawy, H.C. Manning, L.J. Marnett, A. Scilimati, PET radiotracer [^{18}F]-P6 selectively targeting COX-1 as a novel biomarker in ovarian cancer: preliminary investigation, Eur. J. Med. Chem. 80 (2014) 562–568.
[3] J.M. Schwab, R. Beschorner, R. Meyermann, F. Gözalan, H.J. Schluesener, Persistent accumulation of cyclooxygenase-1-expressing microglial cells and macrophages and transient upregulation by endothelium in human brain injury, J. Neurosurg. 96 (2002) 892–899.
[4] O. Pepicelli, E. Fedele, M. Berardi, M. Raiteri, G. Levi, A. Greco, M.A. Ajmone-Cat, L. Minghetti, Cyclooxygenase-1 and -2 differently contribute to prostaglandin E_2 synthesis and lipid peroxidation after in vivo activation of N-methyl-d-aspartate receptors in rat hippocampus, J. Neurochem. 93 (2005) 1561–1567.
[5] R. Calvello, M.A. Panaro, M.L. Carbone, A. Cianciulli, M.G. Perrone, P. Vitale, P. Malerba, A. Scilimati, Novel selective COX-1 inhibitors suppress neuro-inflammatory mediators in LPS-stimulated N13 microglial cells, Pharmacol. Res. 66 (2012) 137–148.
[6] E. Candelario-Jalil, A.C. de Oliveira, S. Gräf, H.S. Bhatia, M. Hüll, E. Muñoz, B.L. Fiebich, Resveratrol potently reduces prostaglandin E2 production and free radical formation in lipopolysaccharide-activated primary rat microglia, J. Neuroinflamm. 4 (2007) 25–37.
[7] S.H. Choi, R. Langenbach, F. Bosetti, Genetic deletion or pharmacological inhibition of cyclooxygenase-1 attenuate lipopolysaccharide-induced inflammatory response and brain injury, FASEB J. 22 (2008) 1491–1501.
[8] J.R. Barrio, N. Satyamurthy, S. Huang, A. Petric, G.W. Small, V. Kepe, Dissecting molecular mechanisms in the living brain of dementia patients, Acc. Chem. Res. 42 (2009) 842–850.
[9] M.G. Perrone, D.D. Lofrumento, P. Vitale, F. De Nuccio, V. La Pesa, A. Panella, R. Calvello, A. Cianciulli, M.A. Panaro, A. Scilimati, Selective Cyclooxygenase-1 inhibition by P6 and gastrotoxicity: preliminary investigation, Pharmacology (2015) 22–28.
[10] L. Di Nunno, P. Vitale, A. Scilimati, S. Tacconelli, P. Patrignani, Novel synthesis of 3,4-diarylisoxazole analogues of valdecoxib: reversal cyclooxygenase-2 selectivity by sulfonamide group removal, J. Med. Chem. 47 (2004) 4881–4890.
[11] M.G. Perrone, P. Vitale, P. Malerba, A. Altomare, R. Rizzi, A. Lavecchia, C. Di Giovanni, E. Novellino, A. Scilimati, Diarylheterocycle core ring features effect in selective COX-1 inhibition, Chem. Med. Chem. 7 (2012) 629–641.
[12] P. Vitale, M.G. Perrone, P. Malerba, A. Lavecchia, A. Scilimati, Selective COX-1 inhibition as a target of theranostic novel diarylisoxazoles, Eur. J. Med. Chem. 74 (2014) 606–618.
[13] V.S. Kristi, A.W. Barbara, Trends in Cancer Therapy: Role of Monoclonal Antibodies, Sem. Oncol. Nurs. 19 (2003) 169–209.
[14] D.R. Buckle, D.J. Outred, C.J.M. Rockell, H. Smith, B.A. Spicer, Studies on 1,2,3-triazoles. (Piperazinylalkoxy)-[1]-benzopyrano-[2,3-d]-1,2,3-triazol-9(1H)-ones with combined H1-antihistamine and mast cell stabilizing properties, J. Med. Chem. 29 (1986) 2262–2267.
[15] M.J. Genin, D.A. Allwine, D.J. Anderson, M.R. Barbachyn, D.E. Emmert, S.A. Garmon, D.R. Graber, K.C. Grega, J.B. Hester, D.K. Hutchinson, J. Morris, R.J. Reischer, C.W. Ford, G.E. Zurenko, J.C. Hamel, R.D. Schaadt, D. Stapert, B.H. Yagi, Substituent effects on the antibacterial activity of nitrogen-carbon-linked (azolylphenyl)oxazolidinones with expanded activity against the fastidious gram-negative organisms Haemophilus influenzae and Moraxella catarrhalis, J. Med. Chem. 43 (2000) 953–970.
[16] J. Imanishi, Y. Morita, E. Yoshimi, K. Kuroda, T. Masunaga, K. Yamagami, M. Kuno, E. Hamachi, S. Aoki, F. Takahashi, K. Nakamura, S. Miyata, Y. Ohkubo, S. Mutoh, Pharmacological profile of FK881 (ASP6537), a novel potent and selective cyclooxygenase-1 inhibitor, Biochem. Pharmacol. 82 (2011) 746–754.
[17] S.P. Bathula, R. Vadla, Bioactivity of 1, 4-Disubstituted-1,2,3-Triazoles as cytotoxic agents against the various Human Cell Lines, Asian J. Pharm. Clin. Res. 4 (2011) 66–67.
[18] G. Cruciani, P. Crivori, P.A. Carrupt, B. Testa, Molecular Fields in quantitative structure-permeation relationships: the VolSurf approach, Theochem 503 (2000) 17–30.

[19] The VolSurf+ Manual available at: http://www.moldiscovery.com/docs/vsplus/.
[20] H.C. Kolb, K.B. Sharpless, The growing impact of click chemistry on drug discovery, Drug Discov. Today 8 (2003) 1128–1137.
[21] F. Wuest, X. Tang, T. Kniess, J. Pietzsch, M. Suresh, Synthesis and cyclooxygenase inhibition of various (aryl-1,2,3-triazole-1-yl)-methanesulfonylphenyl derivatives, Bioorg. Med. Chem. 17 (2009) 1146–1151.
[22] P. Vitale, S. Tacconelli, M.G. Perrone, P. Malerba, L. Simone, A. Scilimati, A. Lavecchia, M. Dovizio, E. Marcantoni, A. Bruno, P. Patrignani, Synthesis, pharmacological characterization and docking analysis of a novel family of diarylisoxazoles as highly selective COX-1 inhibitors, J. Med. Chem. 56 (2013) 4277–4299.
[23] Y. Bourne, H.C. Kolb, Z. Radi, K.B. Sharpless, P. Taylor, P. Marchot, Freeze-frame inhibitor captures acetylcholinesterase in a unique conformation, Proc. Natl. Acad. Sci. U. S. A. 101 (2004) 1449–1454.
[24] D.R. Buckle, D.J. Outred, C.J. Rockell, H. Smith, B.A. Spicer, Studies on v-triazoles. antiallergic 9-oxo-1*H*,9*H*-benzopyrano[2,3-d]-v-triazoles, J. Med. Chem. 26 (1983) 251–254.
[25] M.F. Mady, G.E.A. Awad, K.B. Jørgensen, Ultrasound-assisted synthesis of novel 1,2,3-triazoles coupled diaryl sulfone moieties by the CuAAC reaction, and biological evaluation of them as antioxidant and antimicrobial agents, Eur. J. M. Chem. 84 (2014) 433–443.
[26] R. Alvarez, S. Velázquez, A. San Felix, S. Aquaro, E.D. Clercq, C.F. Perno, A. Karlsson, J. Balzarini, M.J. Camarasa, 1,2,3-Triazole-[2′,5′-bis-O-(tert-butyldimethylsilyl)-beta-D-ribofuranosyl]-3′-spiro-5″-(4″-amino-1″,2″-oxathiole-2″,2″-dioxide) (TSAO) analogues: synthesis and anti-HIV-1 activity, J. Med. Chem. 37 (1994) 4185–4194.
[27] Y.S. Sanghvi, B.K. Bhattacharya, G.D. Kini, S.S. Matsumoto, S.B. Larson, W.B. Jolley, R.K. Robins, G.R. Revankar, Growth inhibition and induction of cellular differentiation of human myeloid leukemia cells in culture by carbamoyl congeners of ribavirin, J. Med. Chem. 33 (1990) 336–344.
[28] M. Journet, D. Cai, J.J. Kowal, R.D. Larsen, Highly efficient and mild synthesis of variously 5-substituted-4-carbaldehyde-1,2,3-triazole derivatives, Tetrahedron Lett. 42 (2001) 9117–9118.
[29] M.D. Chen, S.J. Lu, G.P. Yuag, S.Y. Yang, X.L. Du, Synthesis and antibacterial activity of some heterocyclic β-enamino ester derivatives with 1,2,3-triazole, Heterocycl. Comm. 6 (2000) 421–426.
[30] S. Shafi, M.M. Alam, N. Mulakayala, C. Mulakayala, G. Vanaja, A.M. Kalle, R. Pallu, M.S. Alam, Synthesis of novel 2-mercapto benzothiazole and 1,2,3-triazole based bis-heterocycles: their anti-inflammatory and anti-noceptive activities, Eur. J. Med. Chem. 49 (2012) 324–333.
[31] N. Upmanyu, J.K. Gupta, K. Shah, P. Mishra, Synthesis of new 1,2,4-triazoles as anti-inflammatory and anti-nociceptive agents, Pharm. Chem. J. 45 (2011) 433–439.
[32] K.M. Banu, A. Dinakar, C. Ananthanarayanan, Synthesis, characterization, antimicrobial studies and pharmacological screening of some substituted 1,2,3-triazoles, Indian J. Pharm. Sci. 4 (1999) 202–205.
[33] L.P. Guan, Q.H. Jin, G.R. Tian, K.Y. Chai, Z.S. Quan, Synthesis of some quinoline-2(1H)-one and 1,2,4-triazol-[4,3-a]-quinoline derivatives as potent anticonvulsants, J. Pharm. Pharm. Sci. 10 (2007) 254–262.
[34] A. Passannanti, P. Diana, P. Barraja, F. Mingoia, A. Lauria, G. Cirrincione, Pyrrolo [2,3-*d*][1,2,3]triazoles as potential antineoplastic agents, Heterocycles 48 (1998) 1229–1235.
[35] M. Jilino, F.G. Stevens, Antitumour polycyclic acridines. Part 5. Synthesis of 7*H*-pyrido[4,3,2-*kl*]acridines with exploitable functionality in the pyridine ring, J. Chem. Soc. Perkin Trans. 1 (1998) 1677–1684.
[36] L. Zhou, A. Amer, M. Korn, R. Burda, J. Balzarini, E. De Clercq, E.R. Kern, P.F. Torrence, Synthesis and antiviral activities of 1,2,3-triazole functionalized thymidines: 1,3-dipolar cycloaddition for efficient regioselective diversity generation, Antivir. Chem. Chemother. 16 (2005) 375–383.
[37] C.G. Fortuna, V. Barresi, G. Berellini, G. Musumarra, Design and synthesis of trans 2-(furan-2-yl)vinyl heteroaromatic iodides with antitumour activity, Bioorg. Med. Chem. 16 (2008) 4150–4159.
[38] L. Di Nunno, A. Scilimati, Decomposition of arylazides by THF/*n*-butyllithium-II-isolation of 1-aryl-4,5-dihydro-5-hydroxy-1*H*-1,2,3-triazoles, Tetrahedron 42 (1986) 3913–3920.
[39] P. Vitale, A. Scilimati, Five-membered ring heterocycles by reacting enolates with dipoles, Curr. Org. Chem. 17 (2013) 1986–2000.
[40] P. Vitale, A. Scilimati, Functional 3-arylisoxazoles and 3-aryl-2-isoxazolines from reaction of aryl nitrile oxides and enolates: synthesis and reactivity, Synthesis 45 (2013) 2940–2948.
[41] J. Das, S.N. Patil, R. Awasthi, C.P. Narasimhulu, S. Trehan, An easy access to aryl azides from aryl amines under neutral conditions, Synthesis 11 (2005) 1801–1806.
[42] J.J. Talley, Selective inhibitors of cyclooxygenase-2 (COX -2), Prog. Med. Chem. 36 (1999) 201–234.
[43] T. Liu, X. Dong, N. Xue, R. Wu, Q. He, B. Yang, Y. Hu, Synthesis and biological evaluation of 3,4-diaryl-5-aminoisoxazole derivatives, Bioorg. Med. Chem. 17 (2009) 6279–6285.
[44] K.D. Grimes, A. Gupte, C.C. Aldrich, Copper(II)-catalyzed conversion of aryl/heteroaryl boronic acids, boronates, and trifluoroborates into the corresponding azides: substrate scope and limitations, Synthesis 9 (2010) 1441–1448.
[45] A. Da Settimo, O. Livi, G. Biagi, G. Primofiore, G. Masoni, 1,2,3-Triazole derivatives of aryloxyalanoic acids, Farm. Sci. 37 (1982) 728–739.
[46] P. Crivori, G. Cruciani, P.A. Carrupt, B. Testa, Predicting blood-brain barrier permeation from three-dimensional molecular structure, J. Med. Chem. 43 (2000) 2204–2216.
[47] G. Cruciani, M. Meniconi, E. Carosati, I. Zamora, R. Mannhold, VOLSURF: a tool for drug ADME-properties prediction, in: Drug Bioavailability. Estimation of Solubility, Permeability and Absorption, Meth. and Princ. in Med. Chem, vol. 18, Wiley-VCH publishers, 2003, pp. 406–419.
[48] G. Berellini, G. Cruciani, R. Mannhold, Pharmacophore, drug metabolism, and pharmacokinetics models on non-peptide angiotensin ii AT1, AT2 and mixed AT1/AT2 receptor antagonists, J. Med. Chem. 48 (2005) 4389–4399.
[49] R. Mannhold, G. Berellini, E. Carosati, P. Benedetti, Use of MIF-based VolSurf descriptors in physicochemical and pharmacokinetic studies, in: G. Cruciani (Ed.), Molecular Interaction Fields in Drug Discovery, vol. 27, Wiley-vch Verlag GmbH & Co. KGaA, Weinheim, 2005, pp. 173–193.
[50] S. Wold, M. Sjöström, in: B.R. Kowalski (Ed.), Chemometrics: Theory and Application, ACS Symposium Series, Washington, 1977, pp. 243–282.
[51] S. Wold, C. Albano, W.J. Dunn III, U. Edlund, K. Esbensen, P. Geladi, S. Hellberg, E. Johansson, W. Lindberg, M. Sjöström, Multivariate data analysis in chemistry, in: B.R. Kowalski (Ed.), Chemometrics: MaThematics and Statistics in Chemistry, 1984, pp. 17–96.
[52] V. Barresi, C. Bonaccorso, G. Consiglio, L. Goracci, N. Musso, G. Musumarra, C. Satriano, C.G. Fortuna, Modeling, design and synthesis of new heteroaryl ethylenes active against MCF-7 breast cancer cell-line, Mol. Biosyst. 9 (2013) 2426–2429.